

An IM Driving Power Electronic System Simulation using DNT and Simulink

DNT와 Simulink를 이용한 유도전동기 구동용 전력전자 시스템 시뮬레이션

Moon-Ho Kang
(강 문 호)

요 약 : 교류전동기 구동을 위한 산업용 전력전자 시스템은 전력회생용 양방향 컨버터, VVVF 인버터, 교류전동기 벡터제어기, 및 다양한 전기·기계적 연계 장치들을 포함하는 전기기계 복합시스템 특성을 지니기 때문에 전체 시스템에 대한 컴퓨터 시뮬레이션이 용이하지 않다. 일반적으로 이러한 복잡성을 해결하기 위한 방안으로서 시스템을 근사화 시키고 이에 대한 수학적인 등가모델을 유도한 후 이를 이용하여 시뮬레이션을 행하고 있지만, 이 경우 실제통의 다이 나믹특성을 정확히 표현할 수 없기 때문에 시뮬레이션 신뢰성이 저하될 수 있다. 본 논문에서는 가변구조 제어기법에 의해 역률1 제어기능을 갖는 PWM 컨버터, VVVF 인버터 및 유도기 간접벡터제어기 등을 포함하는 유도전동기 구동 전력전자 시스템을 다이 나믹 노드 기법(Dynamic Node Technique: DNT)과 시뮬링크(Simulink)를 이용하여 실제회로 구성상태와 유사한 형태로 시뮬링크 윈도우상에서 설계하고, 이를 통해 시뮬레이션을 행할 수 있는 기법을 제시한다. 시뮬레이션 결과를 통하여 전력전자 시스템의 특성과 제시된 다이 나믹 노드 기법과 시뮬링크를 이용한 시뮬레이션 기법의 유용성을 보였다.

Keywords : inverter, converter, induction motor(IM), variable structure control scheme(VSCS), dynamic node technique(DNT), Simulink

I. Introduction

Computer-based simulation is an essential element in the design process of industrial ac motor driving power electronic system. Designers of the special power electronic system use simulation techniques to predict and analyze the system requirements using various system parameters. Because real scale field test of high power and large scale power electronic systems such as electric train power converting system or electric power distribution system is usually very time and cost consuming, computer-based pre-examinations or simulations are very effective in view of time and cost saving.

The industrial ac motor driving power electronic system, however, is a complex electromechanical system which includes (bi-directional) converter, VVVF inverter, ac motor vector controller, and many electromechanical interface components. From this complexity computer-based simulation of the entire ac motor driving system is usually so difficult that some approximations and pre-developed mathematically equivalent models are often used in simulation. And this approximations and mathematical models can degrade simulation reliability.

This paper addresses a simulation technique using a topologically similar model for an induction motor (IM) driving power electronic system. The topologically similar model is derived by the Dynamic Node Technique (DNT)[1] and Simulink[2], and the model

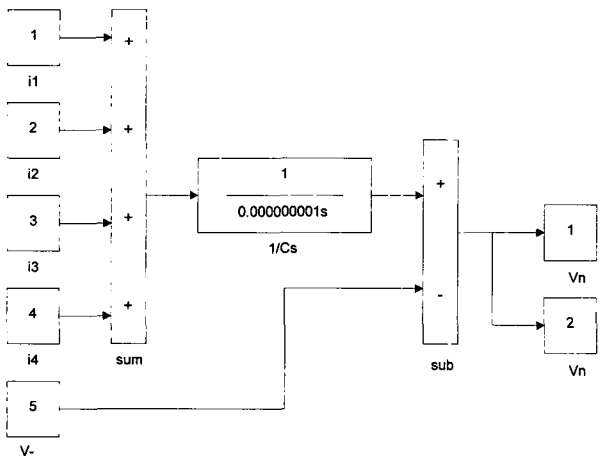
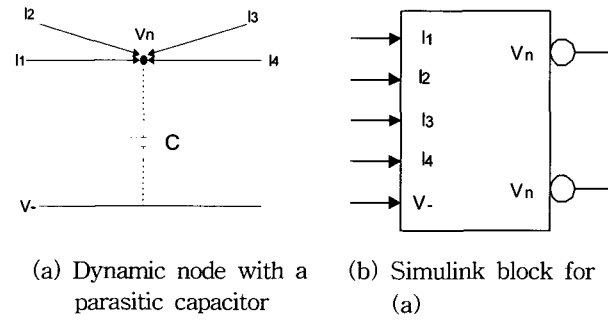
is graphically constructed and simulated on the Simulink window. By the DNT and Simulink-based modeling technique, elementary devices (such as resistor, inductor, capacitor, diode and gate controlled switching devices) can be independently modeled and blocked into power electronic equipment models (such as rectifier, 4 quadrant converter, VVVF inverter and etc.). And this makes it very easy to arbitrarily construct and change the system configuration without any kinds of simulation program codings.

A power electronic system which is modeled with DNT in this paper consists of a unity power factor PWM converter[3][4], a VVVF inverter and an IM indirect vector controller.[5] The PWM converter is controlled by the Variable Structure Control Scheme (VSCS)[6]-[8] and IM speed and current are controlled by the conventional digital PID controllers.

From the simulation results, the proposed system performance and high effectiveness of the simulation technique were verified.

II. Dynamic node technique (DNT)[1]

In the DNT, it is assumed that an imaginary parasitic capacitor is located at a dynamic node which is produced by links of electric devices. This capacitor charges input and output currents of the node. In transient state the difference between the input and output currents flows into the capacitor, but in steady state these currents are balanced, then capacitor current becomes zero, and the node voltage becomes constant. (1) calculates this charging voltage at a dynamic node and Fig. 1 shows its Simulink



(c) Simulink model for (a) (internal config. of (b))

Fig. 1. Dynamic node (a), its Simulink block (b) and Simulink model (c).

model.

Generally the imaginary parasitic capacitor is set to be very small. However, to get simulation result which is more close to real situation the imaginary parasitic capacitor needs to be selected with consideration of the actual electric parasitic charging situation.

Fig. 2 shows an example of DNT model of a R-C series circuit with a voltage source. Each passive device (R and C) is equalized to a block which produces current (i1) into the node block or sinks current (i2) from the node block according to the voltage difference (V1-V2) between the node and each device, while a node acts as an interface block which charges these currents difference through the parasitic capacitor. Like this way it becomes possible to model simulation circuit topologically similar to the real circuit

The switching device modeling process is as follows: A switching device is equalized to two parallel resistors (\$R_{on}\$ and \$R_{off}\$) which respectively have the same values as on and off resistances of the device. And one of these two resistors is selected according to proper driving conditions.

$$V_n = \frac{1}{C} \int \sum I_n dt \quad (1)$$

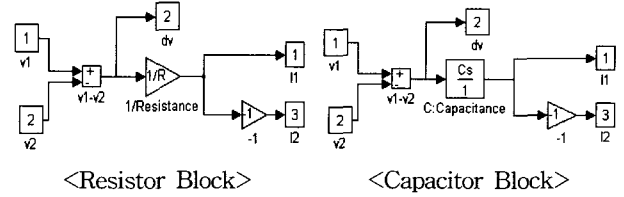
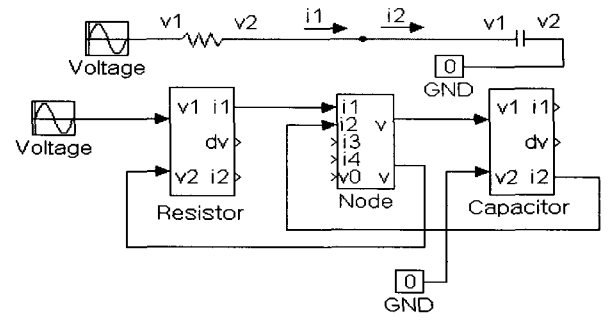
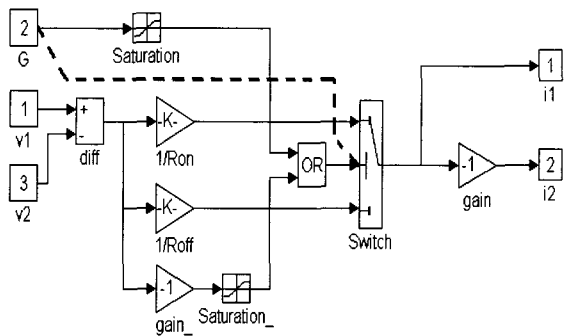


Fig. 2. Simulink model of a R-C series circuit.

Fig. 3 (a) shows an on-off resistors-equivalent model for a power switching device which has an additional anti-parallel diode. In consideration of the combined switching logics of a switching device and an anti-parallel diode, a power switching device can be equivalent to \$R_{on}\$ when gate signal is triggered or \$V2\$ is larger than \$V1\$, and \$R_{off}\$ when otherwise. According to this combined switching logics Simulink model of Fig. 3 (b) can be produced.

(a) On-off resistors-equivalent model of a power switching device



(b) Simulink model of a power switching device

Fig. 3. On-off resistors-equivalent model and Simulink model of a power switching device.

III. Example of ac motor driving power electronic system—ac electric train power converting system

A general form of a power converting system of an ac electric train is shown in Fig. 4. In this system input ac power is collected from a pantograph and filtered through a line ac filter. This filtered input power is transformed through a main transformer, then supplied to a 4 quadrant PWM converter. The PWM converter and a output dc filter make filtered dc link voltage with unity input power factor. Afterward, a VVVF inverter inverts the dc link voltage into ac 3phase sinusoidal voltages, then this voltages drive IM. According to specifically demanded power ratings this system consists of various number of pantographs, converters, inverters and IMs.

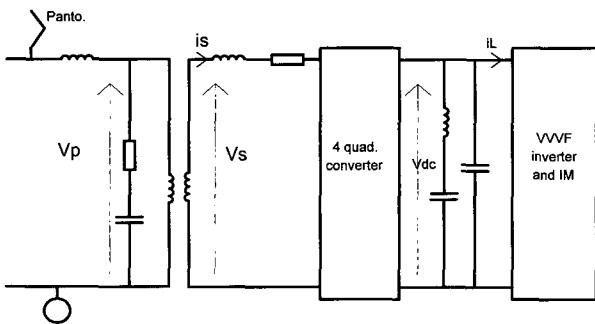


Fig. 4. AC electric train power converting system.

Because major points of this paper are to show not only system performance but also the effectiveness of a DNT-based system modeling and simulation, we constructed a small scale model with a 2.2kw IM. And input ac filter and output dc filter were omitted for the purpose of simplification. And winding ratio of the main transformer was set to be one. System parameters are listed in the Table 2.

The overall control system is modeled and blocked in the Simulink Window as shown in Fig. 5 which consists of 3 main blocks, i.e. PANTO block (Pantograph), PWM CON block (unity power factor 4 quadrant PWM converter control system) and VSI&IM block (Voltage Source Inverter and Induction Motor control system).

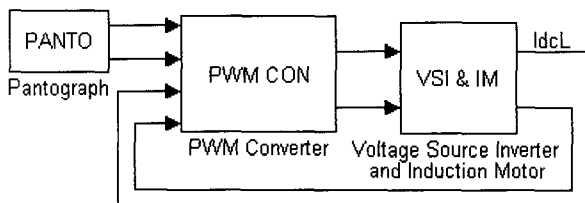


Fig. 5. Overall control system which is modeled and blocked on the Simulink window.

By a click of each block on the Simulink Window, internal block diagram for the each block can be

displayed as shown in Fig. 6-Fig. 10. Fig. 7 represents PWM CONV block in the Fig. 6. In the PWM CONV block, S1-S4 represent power switching devices modeled as Fig. 3. Fig. 7 clearly shows a topologically similar simulation model for a full bridge single phase PWM converter circuit.

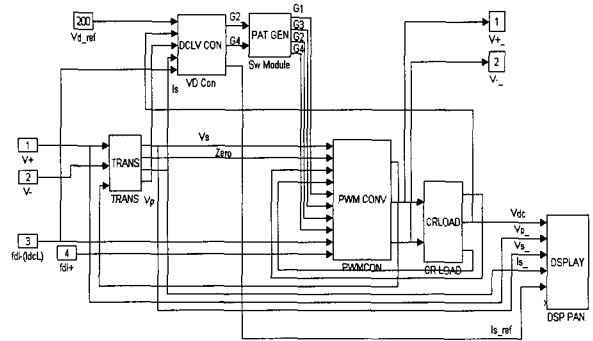


Fig. 6. Simulink model of a PWM converter control system.

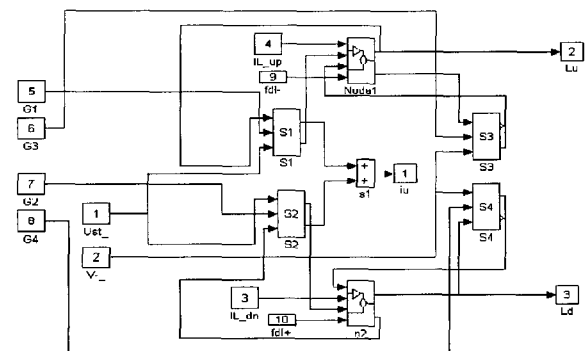


Fig. 7. Simulink model of a PWM converter (PWM CONV in Fig. 6).

1. Modeling a unity power factor PWM converter controlled with VSCS

VSCS is a kind of robust control method realized by discontinuous control input.[6] With VSCS robustness against parameters and disturbances can be obtained by the sliding mode on the switching surface along which state vectors converge toward a stable equilibrium point.

But bearing in mind that VSCS control has a high-frequency discontinuous component (switching) we should consider the problem of correspondence between simulated ideal sliding mode and real-life processes at the presence of unmodeled dynamics in plant models, sensors, actuators.[7] Unlike continuous control the switching in sliding mode control can excite the unmodeled dynamics which is not considered in simulation model and lead to oscillations (chatterings) in the state vectors of the real-life processes. So, to obtain reliable VSCS simulation results, it's very important to model the system dynamics as exactly as possible.

In this paper, because the dominant sub-systems, PWM converter and inverter, are modeled similarly to the topology of real processes, reliable simulation results can be obtained compared with any other mathematically approximated model-based simulations.

For the unity power factor control, converter input current (i_s) must be same phase with input voltage ($v_s = V_m \sin(\omega t + \phi)$). Therefore, for both unity power factor and dc-link voltage (V_{dc}) regulation, converter input current reference (i_s^*) was determined as (2).

$$i_s^* = \left\{ \left(K_P + \frac{K_I}{s} \right) (V_{dc}^* - V_{dc}) + \frac{2 V_{dc}^* i_L}{V_m^2} \right\} v_s = k v_s \quad (2)$$

$$\left[k = \left(K_P + \frac{K_I}{s} \right) (V_{dc}^* - V_{dc}) + \frac{2 V_{dc}^* i_L}{V_m^2} \right]$$

In (2) the first term of the right side is for regulating dc-link voltage to its reference (V_{dc}^*) with a PI regulator. And the second term of the right side is for load current (i_L) compensation. (As being shown from Fig. 4, VVVF inverter and IM acts as a load of converter and its input current becomes a load current for the converter side.)

The load current compensating term in (2) can be obtained as follows. : If unity power factor and ideal dc-link voltage regulation are implemented in steady state and power dissipation of converter is very small compared with load power dissipation, then converter input power is approximated to be equal to load power, namely inverter input power. Thus, (3) can be obtained.

$$v_{srms} i_{srms} \cong V_{dc}^* i_L \quad (3)$$

v_{srms} : rms converter input voltage

i_{srms} : rms converter input current

V_{dc}^* : dc-link voltage reference
(converter output voltage)

i_L : converter load current

From (3), amplitude of converter input current can be determined as (4).

$$I_m \cong \frac{2 V_{dc}^* i_L}{V_m^2} V_m \quad (4)$$

V_m : amplitude of converter input voltage ($\sqrt{2} v_{srms}$)

I_m : amplitude of converter input current ($\sqrt{2} i_{srms}$)

Bearing in mind that converter input voltage and input current have same phase (5) can be obtained from (4). And this result is the same as the last term of (2)

$$i_s = I_m \sin(\omega t + \phi) \quad (5)$$

$$\cong \frac{2 V_{dc}^* i_L}{V_m^2} V_m \sin(\omega t + \phi) = \frac{2 V_{dc}^* i_L}{V_m^2} v_s$$

v_s : instantaneous converter input voltage

i_s : instantaneous converter input current

With the current reference of (2) (i_s^*), the first step of VSCS is to determine switching surface (σ). In this paper σ is set to be the simple form of (6). The second step of VSCS is to make control inputs which satisfy the sliding mode existence condition of (7).

$$\sigma = i_s - i_s^* \quad (6)$$

$$\sigma \frac{d\sigma}{dt} < 0 \quad (7)$$

Considering (7) we can find that following conditions between i_s and di_s/dt should be satisfied.

$$\frac{di_s}{dt} > \frac{di_s^*}{dt} \quad \text{when } i_s < i_s^* \quad \text{ana} \quad (8)$$

$$\frac{di_s}{dt} < \frac{di_s^*}{dt} \quad \text{when } i_s > i_s^*$$

Making control inputs which satisfy above condition can be simply realized by proper driving of converter four switches ($S_1 - S_4$). VSCS-based driving patterns of the four switches can be tabulated as Table 1.[4]

Table 1. VSCS control law for unity power factor PWM converter control.

	$i_s < kv_s$	$i_s > kv_s$
S_1	off	on
S_2	on	off
S_3	on	off
S_4	off	on

2. Modeling an IM vector control system

IM has various merits of maintenance free, high rating and high speed with brushless structure. Especially, because high quality adaptation capability to torque variation can be obtained with vector control method, IM can improve braking and adhesion characteristic of electric trains.

IM vector control system is constructed with IM, VVVF inverter and vector controller[5]. In this paper a VVVF inverter which has switching devices and anti-parallel diodes is modeled with DNT. And PID controllers for decoupling current control and IM speed control are used. A sinusoidal PWM method is used for inverter voltage modulation. IM is represented on the stationary reference frame (Fig. 10). Fig. 8 shows entire IM vector control system modeled on the Simulink window and Fig. 9 is the internal block diagram of the Voltage Source Inverter block (VSI in the Fig. 8).

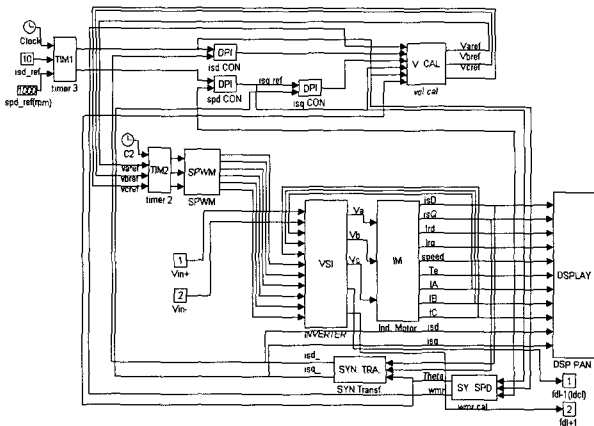


Fig. 8. Simulink model of an IM vector control system.

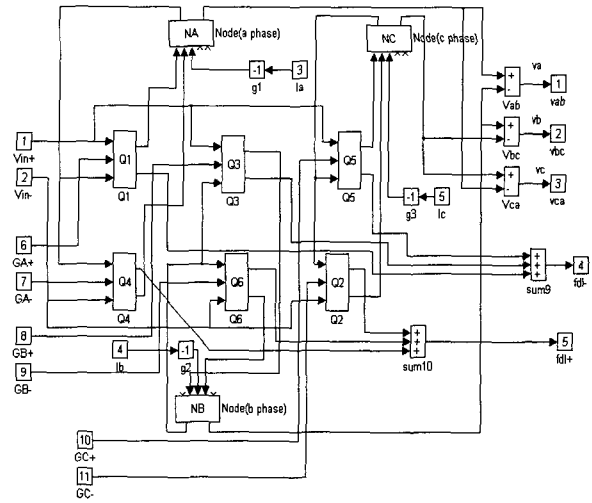


Fig. 9. Simulink model of a VSI in Fig. 8.

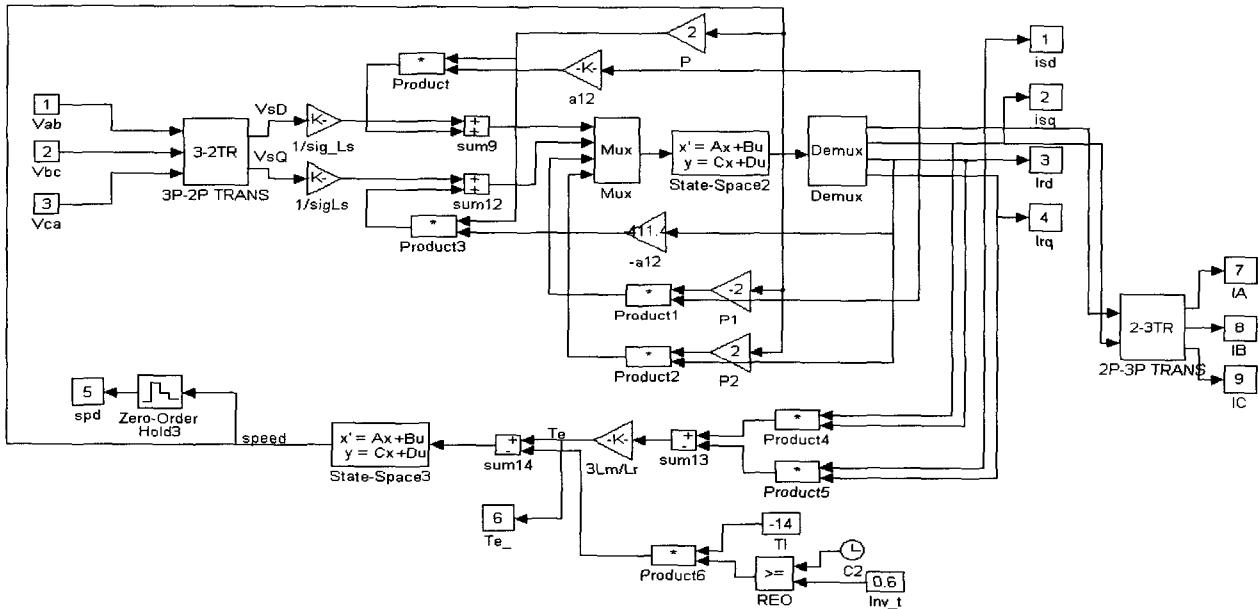


Fig. 10. Simulink model of IM in Fig. 8.

IV. Simulation

With speed reference of 1000 rpm, between 0-0.6 sec IM is set to be driven in powering mode with no load, and between 0.6-0.7sec in regenerating mode with negative full load of -14Nm. Fig. 11 shows speed variation during these time durations. After 0.6sec IM slightly speeds up to 1100 rpm, from this time IM acts as a generator because of the negative load. Fig. 12 shows VSCS current control response where i_s^* is the converter input current reference and i_s is the converter input current. From this figure we can find that the current controlling VSCS is nicely realized. Fig. 13 and Fig. 14 show input voltage (v_s), input current reference (i_s^*) and input current (i_s) of a PWM converter on the same figure.

From these figures it can be shown that unity power factor correction is realized desirably during both powering mode (Fig. 13) and regenerating mode (Fig. 14). Fig. 15. (a) shows dc-link voltage. Dc-link voltage is maintained within $\pm 5\%$ of the reference voltage besides little overshoot in the transient state. The magnified figures of Fig. 15. (a), Fig. 15. (b) and Fig. 15. (c), show characteristic ripple frequency of 120Hz which is inherently induced from the single phase full bridge converter logic. The high ripple voltage is included in the dc link voltage owing to the converter switching action, but this voltage is expected to be effectively removed by the output dc filter. Fig. 16 shows converter input PWM voltage and Fig. 17 shows inverter A-phase current which becomes reverse phase in regenerating mode com-

pared with the case of powering mode. IM and control system parameters are shown in the Table 2.

Table 2. System parameters.

Converter control system	
Input voltage	1 ϕ , 100V, 60Hz
DC-link voltage ref.	200V
Control period	100 μ s
dc-link voltage control gains	$K_p=0.05, K_i=0.15$
BWs of dc-link voltage filter	86Hz
BWs of load current filter	8.6Hz
Input inductance/resistance	2.5mH/0.2 Ω
dc-link capacitance	4000 μ F
IM vector control system	
Ratings : 2.2kW, 3 ϕ , 60Hz, 220V, 14Nm, 1500rpm	
Stator and Rotor resistance	0.345 Ω /0.342 Ω
Stator and Rotor inductance	0.0325H/0.0324H
Magnetizing inductance	0.03132H
Inertia	0.0088kgm ²
Control period	100 μ s
Speed ref.	1000rpm
Load : -14N at 0.6sec (Regeneration)	
Speed control PI gains	$K_p=3, K_i=1$
Current control PI gains	$K_p=5, K_i=1$
PWM carrier frequency	2kHz
DNT parameters	
Parasitic capacitance	10nF
R_{on}, R_{off}	0.1(on)/1M(off) Ω

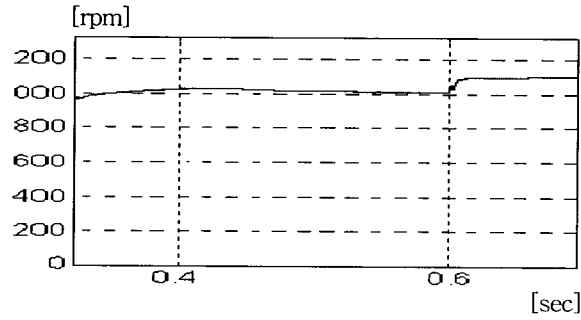


Fig. 11. Speed of IM.

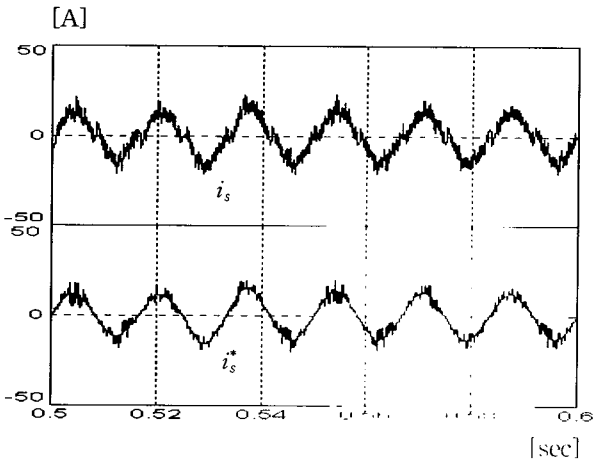


Fig. 12. Converter input current reference (i_s^*) and input current (i_s).

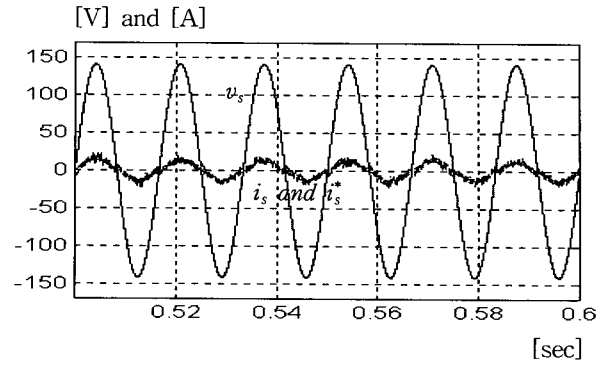


Fig. 13. Converter input voltage (v_s), current (i_s) and current reference (i_s^*) in powering mode.

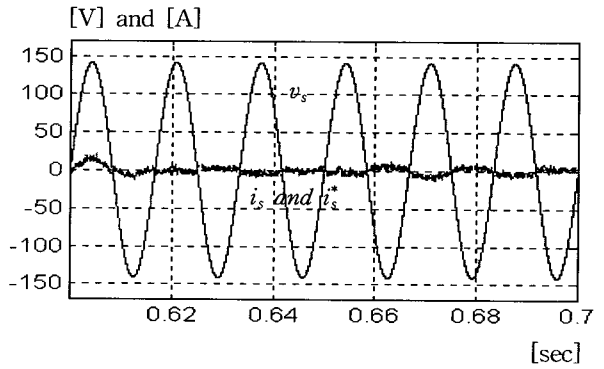
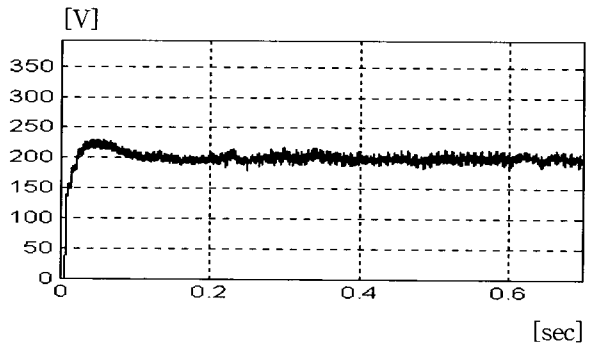
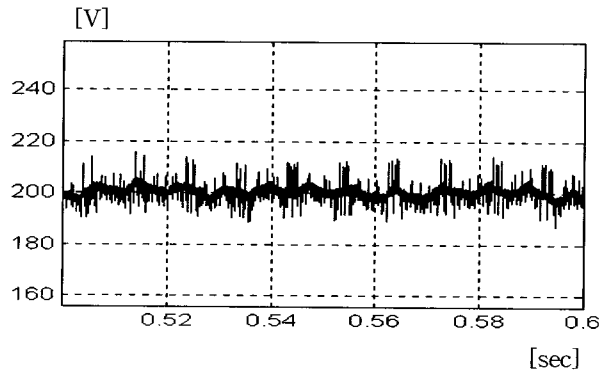


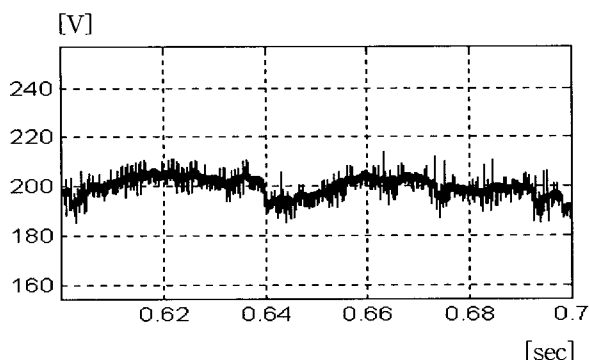
Fig. 14. Converter input voltage (v_s), current (i_s) and current reference (i_s^*) in regenerating mode.



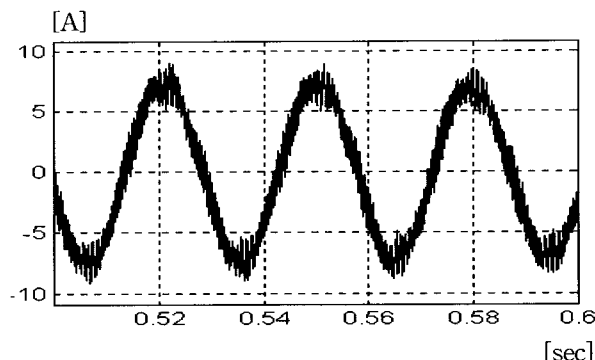
(a) Inverter dc-link voltage over entire control mode



(b) Inverter dc-link voltage in powering mode

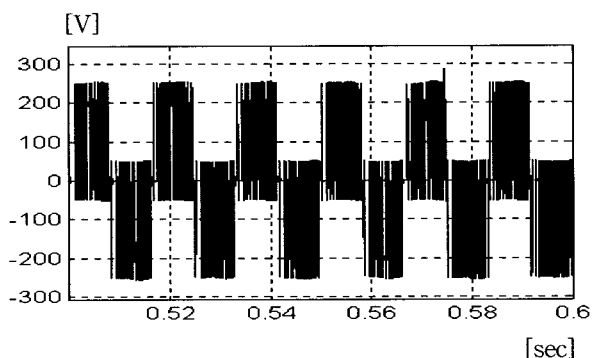


(c) Inverter dc-link voltage in regenerating mode

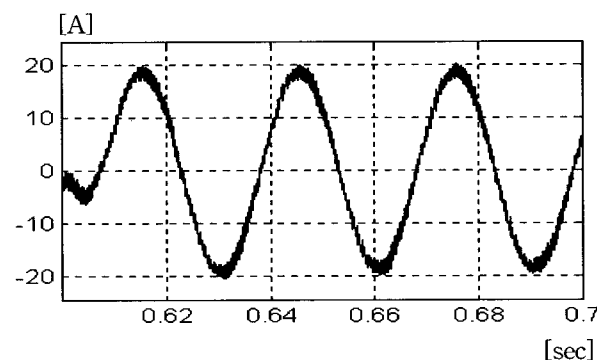


(a) Inverter A-phase current in powering mode

Fig. 15. Inverter dc-link voltage.

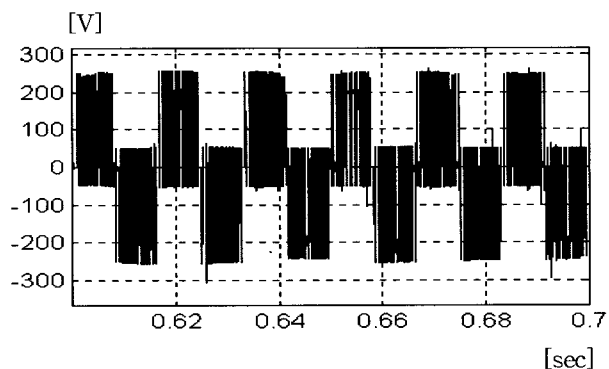


(a) Converter input voltage in powering mode



(b) Inverter A-phase current in regenerating mode

Fig. 17. Inverter A-phase current.



(b) Converter input voltage in regenerating mode

Fig. 16. Converter input PWM voltage.

V. Conclusion

In this paper an induction motor driving power electronic system is modeled and simulated by the DNT and the Simulink. The simulated system consists of a unity power factor PWM converter, VVVF inverter and IM indirect vector controller. With simulation results the desirable performances of the proposed control system could be verified. And it can be proved that DNT and Simulink based simulation technique can be effectively applied to complex power electronic control system. Probably, more accurate

simulation results could be obtained if more actual electric charging conditions are considered in the modeling process. Hereafter, research efforts will be concentrated on the simulation of the real scale electric train power converting system which has unabbreviated system configurations.

References

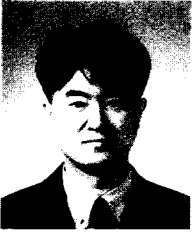
- [1] F. Flinders, S. Senini and W. Oghanna, "Mixed electrical and mechanical simulations using dynamic systems analysis packages," *Proc. of the IEEE-ASME Joint Railroad Conf.*, pp. 87-93, April 1993. pp. 276-280, 1995.
- [2] *Simulink Users Guide*, Math Works Inc., March, 1992.
- [3] T. Takeshita, "Performance of single-phase PWM AC-DC converter with reduced smoothing capacitor," *Proc. of IPEC'95*.
- [4] D. A. Torry et al, "Single phase active power filters for multiple nonlinear loads," *IEEE Trans. on Power Electronics*, vol. 10, no. 3, pp. 263-272, May 1995.
- [5] P. Vas, *Vector Control of AC Machines*, Clarendon Press, Oxford, 1992.
- [6] J. Y. Hung, W. Gao, and J. C. Hung, "Variable structure control : A survey," *IEEE Trans. on Industrial Electronics*, vol. 40, no. 1, pp. 1-22,

Feb. 1993.

- [7] V. I. Utkin, "Sliding mode control design principles and applications to electric drives," *IEEE Trans. on Industrial Electronics*, vol. 40,

no. 1, pp. 23-35, Feb., 1993.

- [8] 이제희, 허욱열, "슬라이딩 제어기법을 이용한 교류 서보시스템의 속도제어," 제어·자동화·시스템 공학회 논문지, 제2권, 제2호, pp. 115-120, 1996. 6.



강 문 호

1988년 고려대 전기공학과 졸업. 동대학원 석사(1990), 동대학원 박사(1995). 한국철도기술연구원 선임연구원(1997). 1997-현재 선문대학교 기계 및 제어공학부 전임강사. 관심분야는 시스템 모델링 및 시뮬레이션,

전동기 지능제어.